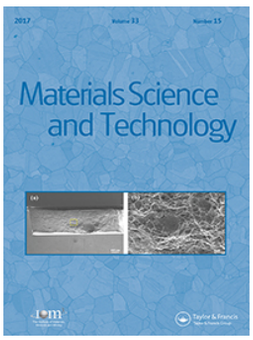

Materials Science and Technology

ISSN: 0267-0836 (Print) 1743-2847 (Online) Journal homepage: https://www.tandfonline.com/loi/ymst20

Medium-manganese steels processed by austenite-reverted-transformation annealing for automotive applications

Yan Ma

To cite this article: Yan Ma (2017) Medium-manganese steels processed by austenite-reverted-transformation annealing for automotive applications, Materials Science and Technology, 33:15, 1713-1727, DOI: 10.1080/02670836.2017.1312208

To link to this article: https://doi.org/10.1080/02670836.2017.1312208

MATERIALS SCIENCE AND TECHNOLOGY, 2017
VOL. 33, NO. 15, 1713–1727
https://doi.org/10.1080/02670836.2017.1312208

The Institute of Materials, Minerals and Mining

Taylor & Francis
Taylor & Francis Group

REVIEW

Medium-manganese steels processed by austenite-reverted-transformation annealing for automotive applications

Yan Ma

Steel Institute, RWTH Aachen University, Aachen, Germany

ABSTRACT

In the automotive industry, the current development trend of lightweight and low-emission vehicles requests for high-performance materials. Benefiting from an excellent balance of mechanical properties and production cost, medium-Mn steels have attracted extensive interest by materials scientists. Austenite-reverted-transformation annealing plays a vital role in stabilisation of retained austenite and grain refinement, resulting in a considerable amount of retained austenite. Localised deformation phenomenon is usually observed in the ultrafine-grained medium-Mn steels owing to the absence of strain hardening. The occurrence of transformation-induced-plasticity and/or twinning-induced-plasticity effect in austenite improves strain hardening effectively. In the current review, austenite-reverted-transformation annealing treatment routine, mechanical properties and deformation mechanisms and effect of heat treatment on microstructure and mechanical properties of medium-Mn steels are summarised.

ARTICLE HISTORY
Received 12 December 2016
Revised 23 March 2017
Accepted 23 March 2017

KEYWORDS
Medium-Mn steels; austenite reverted transformation; transformation-induced plasticity; twinning-induced plasticity; austenite stability; mechanical properties

This review was submitted as part of the 2017 Materials Literature Review Prize of the Institute of Materials, Minerals and Mining run by the Editorial Board of MST. Sponsorship of the prize by TWI Ltd is gratefully acknowledged

1. Introduction

Steel is one of the most important industrial production materials, widely used in the automotive, manufacturing and construction industry. In the last few decades, growing demands of weight saving, emission reduction and passenger safety in the automotive industry have promoted new concepts for modern steel design to achieve an excellent combination of high strength and superior ductility [1–3]. First-generation advanced-high-strength steels (AHSS) have been developed by creating and modifying additional strengthening phases in the ferritic microstructure, like dual-phase (DP) steels, complex-phase (CP) steels, conventional transformation-induced-plasticity (TRIP) steels and martensitic steels [4]. The second-generation AHSS have been intensively studied since the 2000s. The second-generation AHSS are mainly high-manganese steels with austenitic single-phase microstructures. Taking advantage of various deformation mechanisms in high-Mn steels, such as dislocation slipping (SLIP) [5, 6], transformation-induced plasticity (TRIP) [5, 6], twinning-induced plasticity (TWIP) [3, 5, 6] and microband-induced plasticity (MBIP) [5, 6], the second-generation AHSS manifest extreme ductility (total elongation up to 60%) with high strength (ultimate tensile strength up to 1100 MPa). Although the high strength can be achieved in the first-generation AHSS, the ductility is limited. The high amount of alloying content in the second-generation AHSS has raised production cost and created various drawbacks in the production processes [3], for instance, Al_2O_3 formation during casting process, serious macrosegregation and microsegregation due to high carbon and manganese content [7], challenges to hot dip galvanisation because of Al_2O_3 and MnO surface layer formation during continuous annealing [3], etc. The third-generation AHSS has been developed in last two decades to fill the gap between the first-generation AHSS and the second-generation AHSS. The medium-Mn steel grade processed by austenite-reverted-transformation (ART) annealing is one of the most promising candidates in the third-generation AHSS. Compared with the first-generation AHSS, the medium-Mn steels possess raised ductility. The medium-Mn steel additionally takes advantage of lowering the production cost over the second-generation AHSS.

In the 1970s, Miller [8] first developed the medium-Mn TRIP steel with 5.7 wt-% Mn and 0.11 wt-% C. Ultrafine-grained (UFG) duplex microstructure consisting of 10–30 vol.-% austenite with optimised stability was retained by intercritical annealing in the $\gamma+\alpha$ region. The UFG microstructure was a main feature of the medium-Mn TRIP steel, and it had a significantly important effect on the ultra-high strength of medium-Mn steels [8]. However, the UFG microstructure displayed localised deformation behaviour due to the absence of strain hardening [8]. By selection of the

CONTACT Yan Ma yan.ma@iehk.rwth-aachen.de Steel Institute, RWTH Aachen University, Intzestraße 1, Aachen, Germany

optimal ART-annealing temperature, certain amount of austenite phase with desirable stability was successfully retained down to room temperature. During the intercritical annealing, elements such as carbon and manganese partitioned into austenite and stabilised it. As a consequence, the strain hardening rate in the steel was enhanced by the deformation-induced martensite phase transformation, i.e. TRIP effect [8].

The main alloying elements in medium-Mn steels are manganese, carbon, aluminium and silicon. Manganese and carbon are strong austenite stabilisers [9]. The carbon content is generally around 0.05–0.4 wt-% in medium-Mn steels [10–18]. The high carbon content possibly leads to cementite precipitation, and cementite networks could cause intergranular fracture along austenite boundaries [19]. In addition, the high carbon content has a detrimental effect on the weldability of steels, when martensite could form during cooling after welding. In medium-Mn steels, manganese is the most important alloying element, which can effectively stabilise the austenite phase [20, 21]. It usually contains 4–12 wt-% manganese in medium-Mn steels [10–18, 22]. On the one hand, the addition of manganese can lower the A_1 temperature and increase the process window. On the other hand, manganese is intended to increase the hardenability and strongly reduce the critical cooling rate in steels [9]. However, the addition of manganese may also result in poor weldability of steels [9]. Moreover, the manganese concentration in medium-Mn steels is a crucial parameter controlling the deformation mechanisms. Medium-Mn steels with manganese content lower than 9 wt-% were reported to exhibit deformation-induced α'-martensite phase transformation, which were named as medium-Mn TRIP steels [11, 23]. More recently, medium-Mn steels with a higher manganese content from 6 to 12 wt-% were found to reveal successive deformation-induced twinning and α'-martensite transformation during deformation, which are referred to medium-Mn TWIP+TRIP steels [22, 24–27]. The addition of aluminium and silicon in medium-Mn steels is generally around 1.5–3.0 wt-% [10, 22, 25, 26] and 1.2–2.0 wt-% [14, 18, 22, 25], respectively. Interestingly, an improvement in tensile strength and uniform elongation was found in Fe–5Mn–0.1C steel by alloying with 2 wt-% Si [19, 28]. The authors suggested the reduction of dynamic recovery of ferrite by the addition of silicon. Thus, the strain hardening rate could be significantly increased. Suh et al. [18] reported that the addition of up to 3 wt-% Al in medium-Mn steel might lead to the increase in intercritical annealing temperature, but the annealing time could be reduced. In addition, it was reported that addition of Al in Fe–0.08C–6Mn–2Al–1.5Si–0.08 V (wt-%) steel resulted in coarse-grained δ-ferrite in the microstructure [29, 30]. Bimodal grain size distribution of the coarse-grained δ-ferrite and UFG ferrite/austenite can effectively eliminate the localised deformation in medium-Mn steel [29, 30].

According to the enhanced manganese content (>4 wt-%), the classification of steels is listed in Figure 1 [22]. There are two categories, one is the high-Mn steels group with manganese concentrations above 15 wt-%, and the other group is medium-Mn steels with manganese content from 4 to 12 wt-%. As it is illustrated in Figure 1, the microstructure could be tailored by reducing the manganese content from single austenite to UFG duplex ferrite and austenite. It can be seen that the manganese content significantly affects the stacking fault energy (SFE) in austenite and austenite stability and further has an impact on the deformation mechanisms in medium-Mn steels.

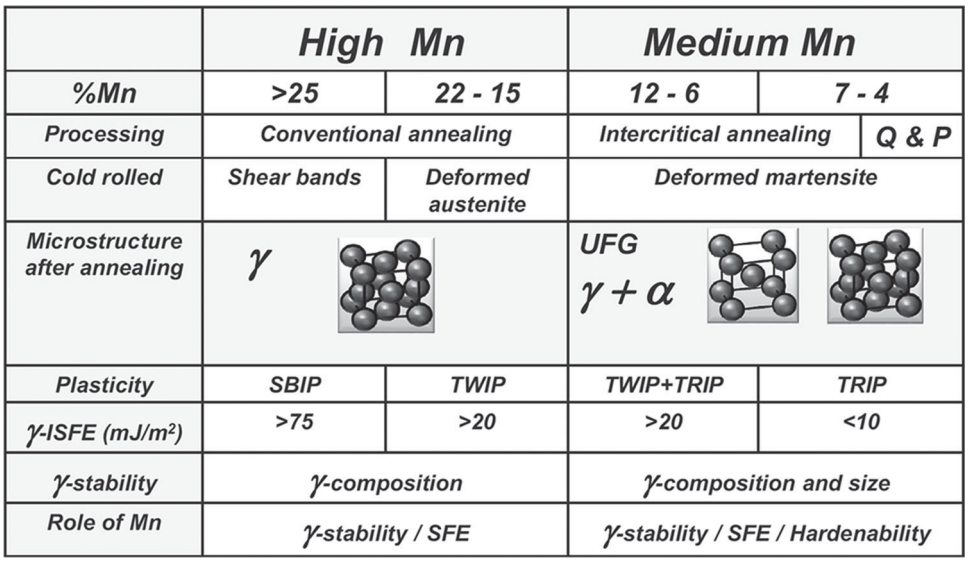

Figure 1. Classification of the types of steels with enhanced manganese content. Q&P: quench and partitioning; UFG: ultrafine-grained; SBIP: shear-band induced plasticity; TWIP: twinning-induced plasticity; TRIP: transformation-induced plasticity; SFE: stacking fault energy [22]. (Reproduced with permission from Wiley-VCH Verlag GmbH & Co. KGaA.).

Recently, numerous studies have been carried out to study the deformation mechanisms [18, 24, 25, 31] in medium-Mn steels and investigate the influence of heat treatment parameters on the microstructure and mechanical properties of medium-Mn steels, in terms of austenitisation temperature [15, 23], annealing temperature [16, 18, 21, 32], annealing time [33–35], heating rate [36], etc. during ART annealing. In this literature review, the phenomenological description of austenite reverted transformation is addressed in the second chapter. Following, the mechanical properties and the deformation behaviour of current medium-Mn TRIP and TWIP+TRIP steels are outlined. In the last part, the influence of heat treatment parameters on the microstructure and mechanical properties is summarised.

2. Austenite-reverted-transformation annealing and austenite stability

For an excellent balance of strength and ductility in medium-Mn steels, a large amount of retained austenite is essential. The ART annealing is a novel concept to refine the microstructure and stabilise retained austenite by carbon and manganese partitioning. The mechanical properties of medium-Mn steels can be greatly affected by the heat treatment routines [37–42].

2.1. Austenite-reverted-transformation annealing

The principle of ART-annealing process is illustrated in Figure 2. First, the steel strip (cold rolled or hot rolled) is heated above A_3 temperature to achieve a fully austenitic microstructure. Subsequently, the austenite fully or partially transforms to α'-martensite by quenching to room temperature, which is closely dependent on the chemical composition of medium-Mn steels [10, 17, 26]. In the medium-Mn TRIP steels with manganese content lower than 9 wt-% athermal martensite is favoured during quenching [10, 23, 34], while certain amounts of retained austenite and/or ferrite might coexist with martensite in as-quenched medium-Mn TWIP+TRIP steels with higher manganese content (Mn >6 wt-%) [17, 26]. Next, the steel strip is reheated to the intercritical annealing temperature between A_1 and A_3 and held isothermally at this evaluated temperature for some time, followed by cooling to room temperature. Alternatively, the conventional rolling and ART-annealing process might be employed to manufacture this steel grade [26]. For instance, hot rolling is possibly conducted above the A_3 temperature in combination with an austenitisation treatment, followed by cold rolling. During the cold rolling process, retained austenite from hot-rolled medium-Mn steels might transform into martensite due to the deformation. It was pointed out that the cold rolling increased the stored energy in steel significantly, which was reported to result in profound nucleation of austenite and rapid elemental partitioning during subsequent intercritical annealing [8]. However, there might be some difficulties to perform a cold rolling directly after austenitisation or the hot rolling process due to the brittle feature of quenched martensite. An intercritical annealing between the hot rolling and the cold rolling could be applied to soften the material, in order to further carry out the cold rolling process. What's more, Zhao et al. [16] reported that hot rolling combined with warm rolling at intercritical temperature could replace the conventional cold rolling and ART-annealing processes. The as-warm-rolled sample

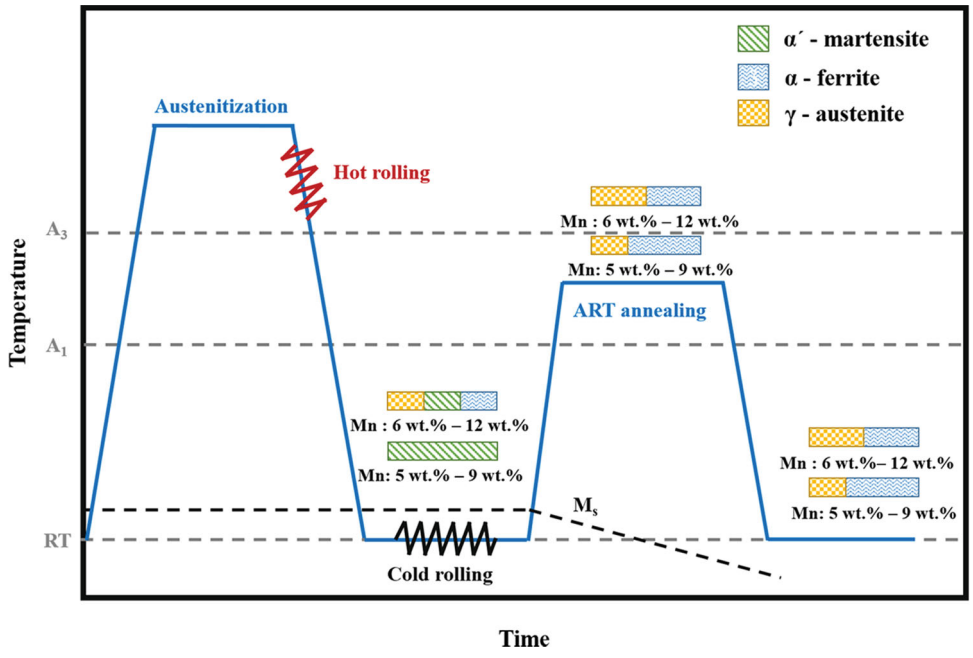

Figure 2. Schematic representation of ART-annealing process.

exhibited comparable mechanical properties with samples produced by conventional three-stage processes, including hot rolling, cold rolling and annealing [16].

During ART annealing, the nucleation of austenite takes place along martensite lath boundaries, martensite block boundaries or primary austenite boundaries [38], leading to a pronounced grain refinement [22]. As a consequence, either UFG duplex microstructures with austenite and ferrite lamella [23, 34], or equiaxed microstructures with ferrite and retained austenite [17, 33], or multi phase microstructures with bimodal distribution (coarse-grained austenite and ultrafine-grained austenite + ferrite [25], or coarse-grained recrystallised ferrite and ultrafine-grained austenite + ferrite [18]) could form in medium-Mn steels. ART annealing resulted in ultrafine grain size of ferrite and austenite, which was reported usually smaller than 1 μm [11, 23, 34]. It was claimed that the ultrafine grain size could effectively improve austenite stability [21, 31, 32, 43]. Also, elemental partitioning during the ART annealing plays the most important role in austenite stabilisation. Manganese and carbon enrichment in austenite during ART annealing lead to a considerable amount of retained austenite after final cooling [32, 35, 44, 45].

2.2. Enhanced austenite stability by ART annealing

Miller [8] has pointed out the fraction of austenite obtained during ART annealing was strongly dependent on the alloying content of the steel and the annealing temperature. According to thermodynamics, the intercritical annealing temperature has a noticeable impact on the amount and stability of austenite. De Moor et al. [20] have proposed a thermodynamic model to predict the dependence of retained austenite fraction as a function of the ART-annealing temperature, as shown in Figure 3. The retained austenite fraction after ART annealing was predicted based on the austenite stability, which was quantified by the martensite start (M_s) temperature. The amount of retained austenite was calculated by subtracting the amount of newly obtained martensite during cooling to room temperature from the total austenite under the equilibrium conditions. The amount of fresh martensite was estimated by the Koistinen-Marburger (KM) equation [20]. As illustrated in Figure 3, a pronounced peak of the retrained-austenite fraction is obtained, indicating the largest amount of retained austenite achieved via ART annealing [20]. The austenite fraction increases with an increase in annealing temperature in the intercritical regime, though the amount of manganese decreases in the austenite phase. The insufficient stabilisation of the austenite phase due to the lower manganese content results in a large amount of newly formed martensite

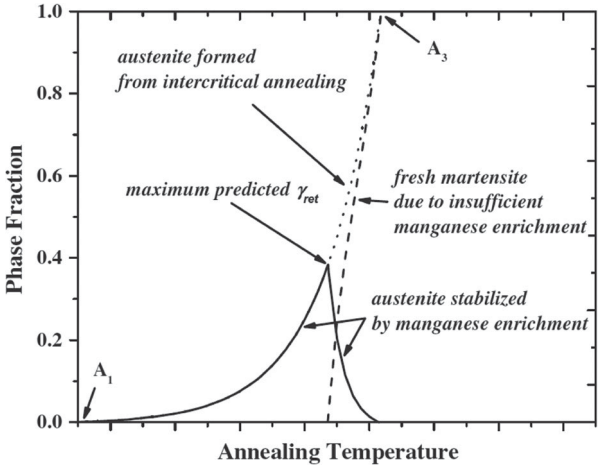

Figure 3. Schematic diagram of stabilised austenite fraction as a function of annealing temperature. The solid line is the fraction of retained austenite, the dotted line is the fraction of austenite formed at the intercritical annealing temperature and the dashed line is the fraction of newly formed martensite during cooling [20]. (Reproduced with permission from Elsevier).

during subsequent cooling. Consequently, the austenite fraction drops with increasing annealing temperature.

An improved thermodynamic prediction was reported by Lee et al. [17, 21, 46] in which the annealing-temperature-dependent grain size was taken into account as well, as illustrated in Figure 4 [17]. The dependence of retained austenite grain size on the annealing temperature is shown in Figure 4(a) [17]. The increasing annealing temperature results in coarsening of retained austenite grain. Figure 4(b) [17] manifests the dependence of the M_s temperature on the annealing temperature and grain size. The M_s temperature decreases with decreasing annealing temperature. Considering the grain size effect, the M_s temperature could be further reduced by the reduction of retained austenite grain size. The volume fraction of austenite, ferrite and martensite at room temperature as a function of annealing temperature is shown in Figure 4(c) [17]. The maximum volume fraction of austenite is obtained after ART annealing at approximately 730°C regardless of the grain size effect on austenite stability. Further increase of the annealing temperature leads to the reduction of retained austenite volume fraction, because α'-martensite forms during the cooling from intercritical annealing temperature. Considering the retained austenite grain size, the formation of martensite is further retarded during cooling. Consequently, the largest amount of retain austenite can be obtained at a higher ART-annealing temperature of 800°C. In comparison, rather more austenite can be retained at the same annealing temperature, if the effect of grain size is taken into account. The SFE as a function of annealing temperature and grain size was calculated by the modified Olson and Cohen model and is displayed in Figure 4(d) [17]. The SFE in retained austenite strongly depends on the annealing temperature. Moreover, it can

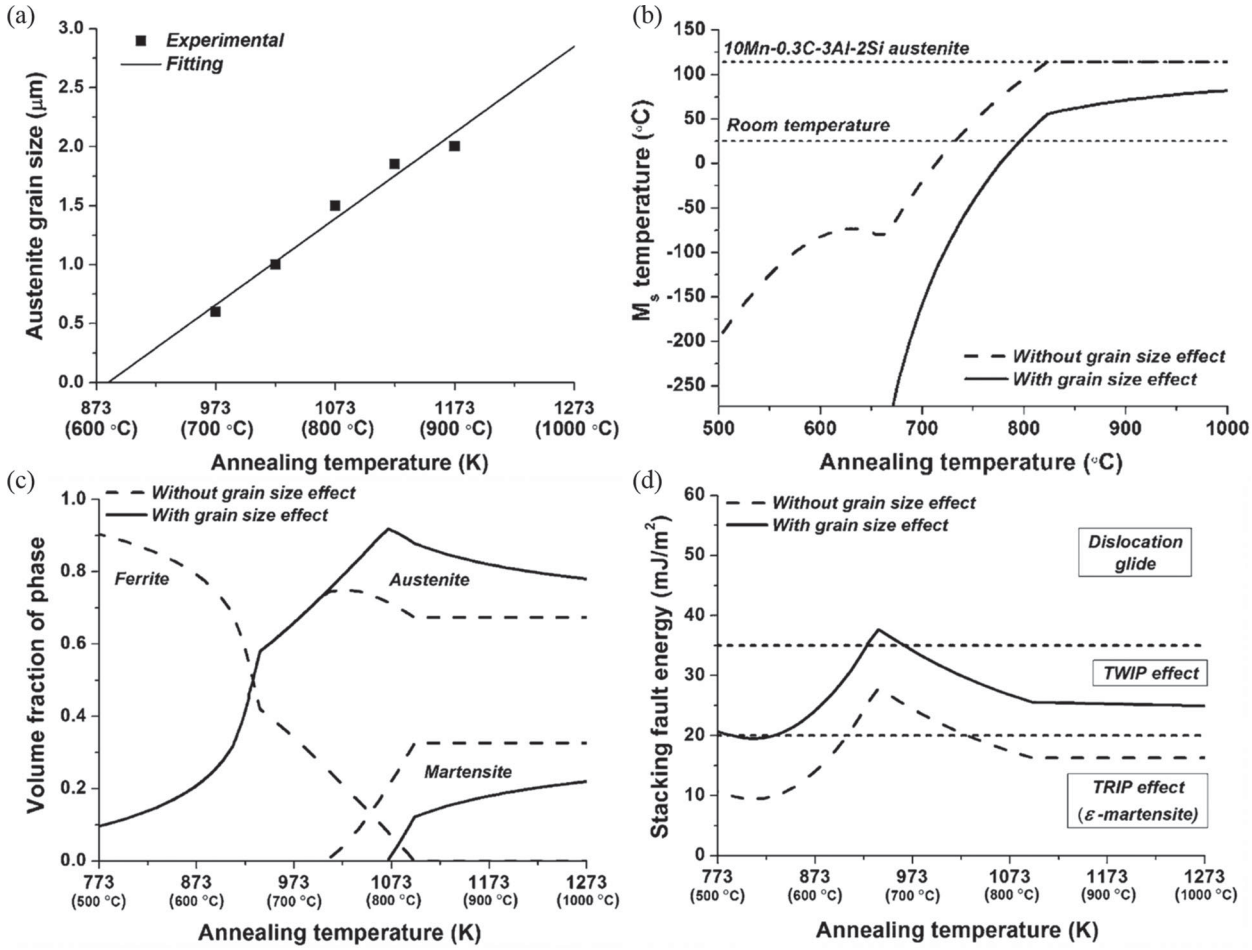

Figure 4. (a) Austenite grain size as a function of annealing temperature; thermodynamic prediction on the dependence of (b) M_S temperature, (c) volume fraction of phase and (d) SFE in retained austenite on the annealing temperature and grain size in Fe–10Mn–0.3C–3Al–2Si (wt-%) steel [17]. (Reproduced with permission from Springer).

be seen that the decrease in grain size increases SFE. It has been indicated that regardless of the chemical stabilisation of austenite, the austenite grain size has a great impact on the austenite stability and SFE in retained austenite [17].

Lee et al. [32, 45] described three main effects that controlled the austenite stability:

- Chemical composition: it is related to the elemental partitioning between austenite and ferrite phases, resulting in stabilised austenite.
- Grain size effect: reduced grain size results in lower martensite transformation start temperature and stabilises austenite.
- Mechanical stabilisation: reversely transformed austenite inherits the high dislocation density feature of the parent martensite, resulting in mechanical stabilisation.

3. Mechanical properties and strengthening mechanisms

The UFG medium-Mn TRIP steel Fe–5.7Mn–0.11C (wt-%) studied by Miller [8] in 1972 revealed excellent mechanical properties (UTS of 1145 MPa and total elongation of 30.5%) with about 30 vol.-% austenite phase. Recently, the development of medium-Mn (4–12 wt-% Mn) steels with various chemical compositions and processing routes has been reported. The mechanical properties concerning ultimate tensile strength and total elongation are visualised in Figure 5. The mechanical properties of the medium-Mn steels are apparently related to the chemical compositions and the heat treatment conditions. It can be seen that the ultimate tensile strength of medium-Mn steels covers a large spectrum; meanwhile the medium-Mn steels exhibit adequate ductility. The ultimate tensile strength and the total elongation are reported in the range of 800–1600 MPa and 10–65%, respectively. Moreover, the medium-Mn steels exhibit high yield/tensile ratio [18, 37, 41], showing a great potential for anti-intrusion automotive part applications. Recently, Lee et al. [24] reported an ultimate tensile strength of 1144 MPa with an elongation of 65% in Fe–10Mn–0.3C–3Al–2Si (wt-%) steel. In comparison to a high-Mn TWIP steel (Fe–18Mn–0.6C–1.5Al, wt-%) [24], the reported mechanical properties of the previous steel grade are superior. It has been claimed that the excellent combination of high strength and superior ductility in medium-Mn steels is attributed to the

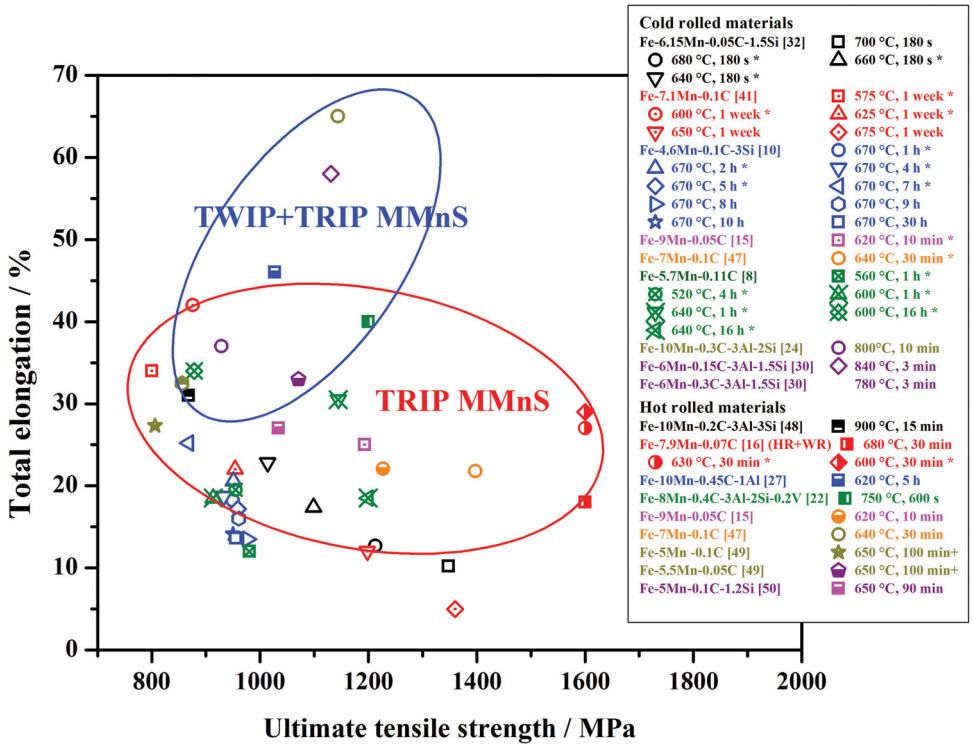

Figure 5. Total elongation vs. ultimate tensile strength in medium-Mn steels under different ART-annealing conditions. (The stress–strain curves showing discontinuous yielding are marked with *; the stress–strain curves not given in the references are marked with $^{+}$).

high strain hardening rate resulting from the TRIP effect [8, 51] or the synergistic effect of TWIP and TRIP [24–27, 48].

3.1. Lüders deformation behaviour

Typically, UFG medium-Mn steels display stress–strain curves with well-defined upper and lower yield points (discontinuous yielding) followed by yield point elongation, which is referred to as Lüders deformation behaviour [32, 52]. The occurrence of this type of localised deformation is undesirable, because it has negative effects on the surface quality of the material. Lüders strain was observed in carbon steels [53]. Interstitial elements such as carbon, nitrogen and boron in steels are proposed to be responsible for this stretching strain by locking dislocations and the formation of Cottrell atmosphere during deformation [54].

The previous study of UFG TRIP steels by Miller [8] claimed that there were three different types of stress–strain curves in UFG steels, as shown in Figure 6 [8]. Type I stress–strain curve features plasticity instability in the form of necking in the deformation band before the band goes through the entire gage of the sample, which means that necking and fracture occur during Lüders deformation [8]. Type II stress–strain curve is characterised by very low strain hardening rate [8]. In the Type III stress–strain curve, an increased strain hardening capacity is observed, which results from the austenite phase transformation into martensite during mechanical deformation [8]. The grain size

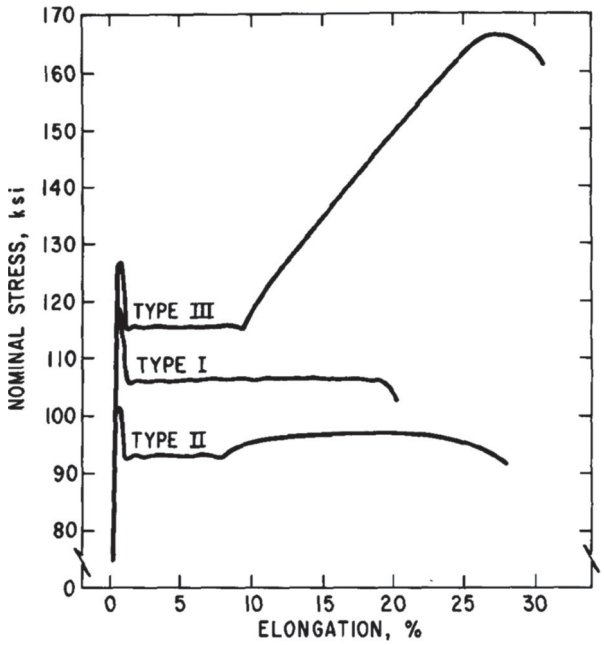

Figure 6. The three different stress–strain curve types discovered in UFG steels [8]. (Reproduced with permission from Springer).

was reported to have a significant effect on the localised deformation. In the UFG steels, when the grain size was smaller than 0.57 μm, the stress–strain curves were reported as Type I [8]. However, the deformation of UFG steel with increased grain size larger than 0.7 μm resulted in stress–strain curve Type II [8].

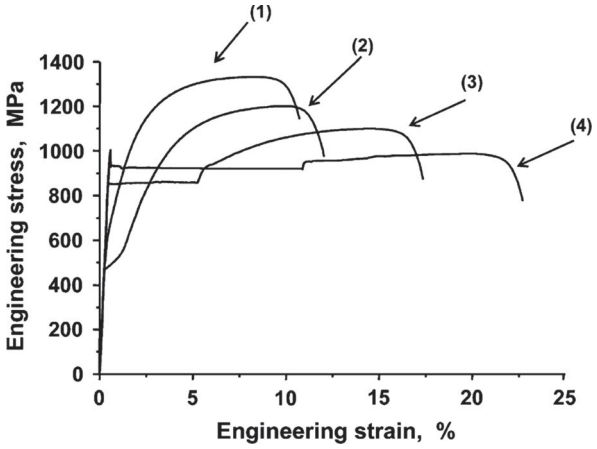

Figure 7. Engineering stress–engineering strain curves of cold-rolled Fe–6wt-%Mn steel samples annealed at different temperatures (1) 700°C, (2) 680°C, (3) 660°C, and (4) 640°C for 180 s [32]. (Reproduced with permission from Springer).

Engineering stress–strain curves of Fe–6wt-%Mn steel are shown in Figure 7, characterised by the profound localised deformation behaviour, especially in the sample annealed at 640 and 660°C [32]. Lüders strain was reported to decrease with the increase of annealing temperature (from 640 to 700°C) in Fe-6wt-% Mn steel. Indications for localised deformation were absent in samples annealed at 700°C. Lee et al. [32] reported that the observation of Lüders deformation behaviour was closely related to the localisation of strains due to the lack of work hardening.

The inverse square root dependence of the Lüders strain on grain size has been observed in the previous study [55]. In other words, with decreasing grain size, more pronounced Lüders strains are expected to occur [32]. However, in the study of localised deformation behaviour of Fe–6wt-%Mn steel [32], the average grain size remained almost constant at 300 nm for all the investigated samples and the effect of grain size on the Lüders strain was intended to be negligible in this case. Interestingly, Lee et al. [32] found that not only the grain size had a great effect of the Lüders strain, but the austenite stability also played an essential role in it. The highly stabilised austenite could not transform into martensite during deformation, i.e. in the sample annealed at 640°C. In contrast, the retained austenite dynamically transformed into martensite in the sample annealed at 680°C, nucleating numerous mobile dislocations. As a consequence, the strain hardening increased substantially, and the Lüders strain was effectively reduced or eliminated by this TRIP effect [32]. Another study [51] suggested that dislocation movement is solely limited in close proximity to grain boundaries of the ferrite phase, once a dislocation was generated from a grain boundary source. The back stress exerted by former generated dislocations strongly hindered the dislocation generation and gliding across the grain, leading to grain boundary thickening [51]. The absence of strain hardening in the sample annealed at 640°C might be related to grain boundary thickening in the ferrite phase and the absence of martensite transformation during deformation in the austenite phase due to its high stability [51]. On the contrary, the combination of TRIP effect in the austenite phase and dislocation interactions in large ferrite grains is supposed to result in the high strain hardening rate in the sample annealed at 680°C [51]. Hence, the control of the austenite stability is of great importance to improve the mechanical properties of medium-Mn steels.

3.2. TRIP and TWIP effects in medium-Mn steels

It is known that the austenitic high-Mn steels in the second-generation AHSS take advantage of both high strength and superior ductility due to the unique strain hardening features [3, 5, 56]. The TRIP effect [5, 6], twinning-induced plasticity (TWIP) effect [6, 56] and microband-induced plasticity (MBIP) effect [6, 57] on the strain hardening behaviour in high-Mn steels have been intensely studied in the last two decades. In order to enhance the strain hardening rate, TRIP and TWIP effect have already been introduced into medium-Mn steels [8, 24].

The strain hardening behaviour of medium-Mn TRIP steels has been reported in 5% Mn steels [11, 13, 18, 37] and 6.15% Mn steels [29, 32]. Wang et al. [11] claimed that during deformation there was no apparent change of the ferrite phase in Fe–5Mn–0.2C steel apart from the slight increase in dislocation density. However, the α'-martensite phase transformation was observed in UFG austenite phase during deformation. Figure 8 displays the engineering stress–strain curve of UFG Fe–5Mn–0.2C steel and the austenite fraction variation during the tensile test [11]. XRD measurements reveal a continuous decrease in austenite from 40 to 0.6 vol.-% with progressive straining up to 0.4, indicating the complete phase transformation of austenite to α'-martensite. Moreover, XRD results confirm the absence of ε-martensite transformation as a transition phase [11].

Recently, Lee et al. [24] found that intercritically annealed 10 wt-% Mn steels exhibited excellent mechanical properties with tensile strength up to 1144 MPa and elongation about 65%. The high strain hardening rate of this steel was reported to be related to the combination of TWIP and TRIP effect occurring progressively during the tensile test. The fraction, grain size, stability and room temperature SFE of austenite were found as critical parameters controlling the strain hardening rate and further mechanical properties in 10 wt-% Mn steels [17, 24, 31]. The intercritical annealing concept and deformation mechanisms in the cold-rolled 10 wt-% Mn steels are illustrated in Figure 9 [24]. Manganese and carbon atoms are supposed to partition into the austenite phase during the intercritical

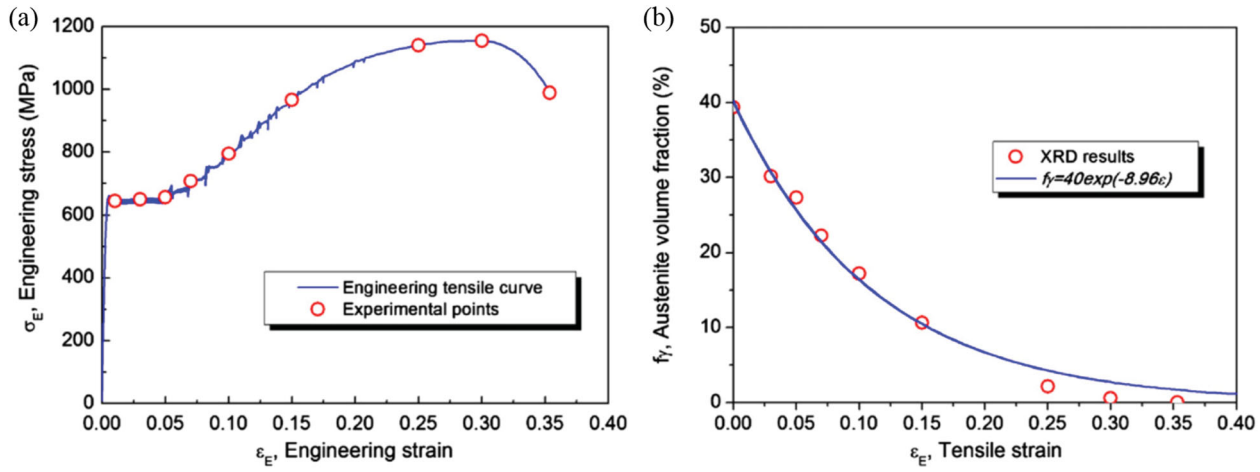

Figure 8. (a) Engineering stress–engineering strain curve and (b) austenite volume fraction evolution during tensile deformation in UFG Fe–5Mn–0.2C (wt-%) medium-Mn steel [11]. (Reproduced with permission from Elsevier).

annealing process to stabilise the retained austenite; on the contrary, silicon and aluminium diffuse to the ferrite phase [24]. Moreover, the room temperature SFE of austenite phase has been considered in this case, which determines the deformation mechanisms [24]. Owing to manganese and carbon partitioning during ART annealing, the SFE of austenite phase is high enough to promote deformation twins during the tensile test. As illustrated in Figure 9 [24], during mechanical deformation primary twins are generated and followed by secondary twins. The twin intersections are intended to be nucleation sites for the following deformation-induced α'-martensite transformation [24].

In the study on the tensile behaviour of medium-Mn Fe–12Mn–0.3C–(2,3)Al (wt-%) multiphase steel by Lee et al. [25], it was observed that ferrite had a rather higher yield strength compared with austenite. However, the *in situ* neutron diffraction results indicated the absence of the strain hardening rate of the ferrite phase. The high strain hardening rate in austenite resulted from deformation-induced twinning and α'-martensite phase transformation. Neutron diffraction experiments confirmed the stacking faults, and deformation twins were generated at the low strain level [25]. In contrast, the deformation-induced α'-martensite transformation occurred at the high strain level. The critical stress to activate martensite transformation was determined to be about 887 MPa for both 2Al and 3Al medium-Mn steels. In conclusion, TWIP and TRIP effects were identified as effective mechanisms to increase of strain hardening behaviour of medium-Mn steels.

In medium-Mn steels, the proper control of the austenite stability is essential to obtain superior mechanical properties [8, 25, 32]. The austenite stability can be controlled by the appropriate adjustment of its chemical composition and grain size as it is mentioned before. Moreover, the SFE is another critical parameter determining deformation mechanisms [17]. The SFE plays a decisive role in the activation of strain-induced martensite transformation or twins during deformation. When the SFE is in the range of 0–20 mJ m^{-2}, TRIP is favoured, while TWIP is preferred when the SFE is in between 20 and 35 mJ m^{-2} [17].

4. Effect of heat treatment process on the microstructure and mechanical properties

As discussed in the previous chapters, stabilisation of retained austenite by ART annealing plays an essential role to achieve desirable mechanical properties. The heat treatment procedure of medium-Mn steels consists of austenitisation and ART annealing, as shown in Figure 2. The heat treatment parameters such as austenitisation temperature and time, ART-annealing temperature and time are of great importance for the microstructure and mechanical properties of medium-Mn steel. In this chapter, the effects of main process parameters on the microstructure, mechanical properties and austenite stability are reviewed.

4.1. The influence of the austenitisation temperature

The austenitisation temperature has a strong influence on the morphology of quenched martensite [15, 23]. This directly affects the austenite reverted transformation, such as the austenite volume fraction, transformation rate and grain size. The average size of packets and widths of blocks increases with increasing austenising temperature [23], as illustrated in Figure 10.

Figure 11 shows the changes in volume fraction, transformation rate and grain size of reverted austenite at different austenising temperatures [23]. The results indicate that the specimen austenitised at the lower temperature has a higher volume fraction of retained austenite. The higher austenitisation temperature leads to coarsening of prior austenite and reduction in the

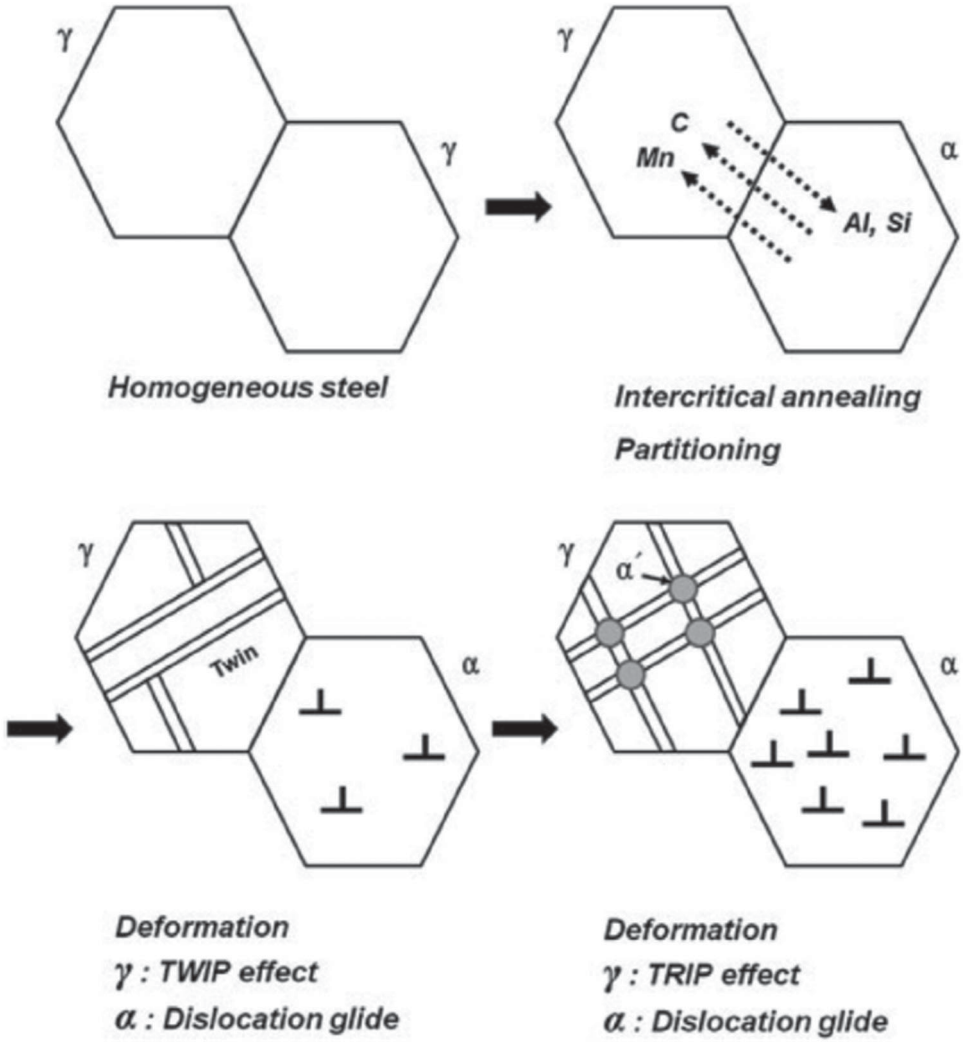

Figure 9. Schematic illustration of intercritical annealing concept and designed deformation mechanisms in 10 wt-% Mn steels [24]. (Reproduced with permission from Springer).

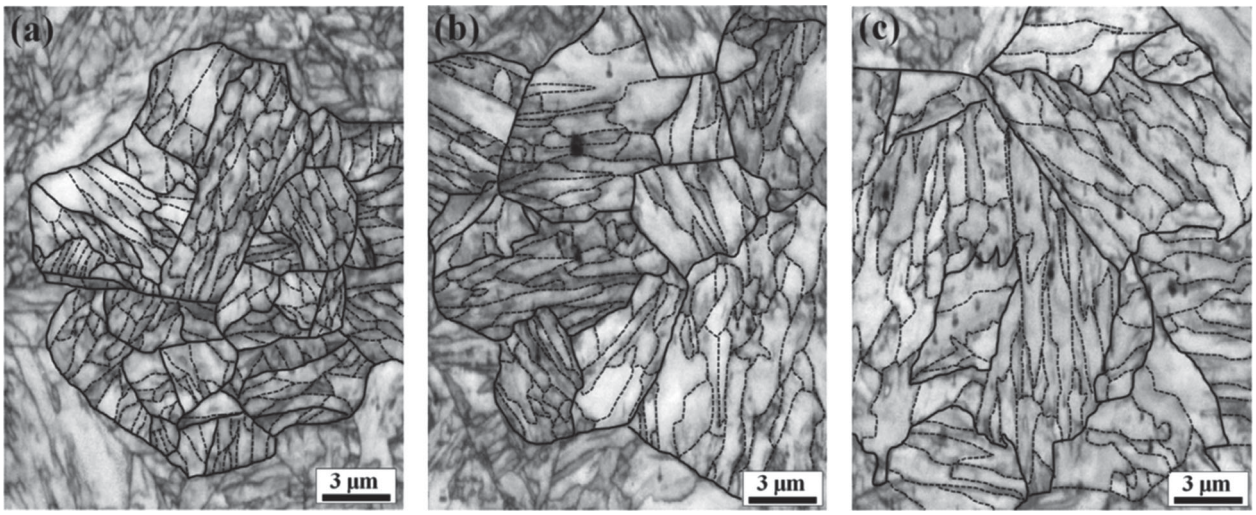

Figure 10. Electron backscatter diffraction image quality maps of quenched martensite phases at various austenitisation temperatures: (a) 800°C, (b) 900°C and (c) 1000°C in Fe–9Mn–0.05C (wt-%) steel. Solid and dashed lines are packet and block boundaries, correspondingly [23]. (Reproduced with permission from Elsevier).

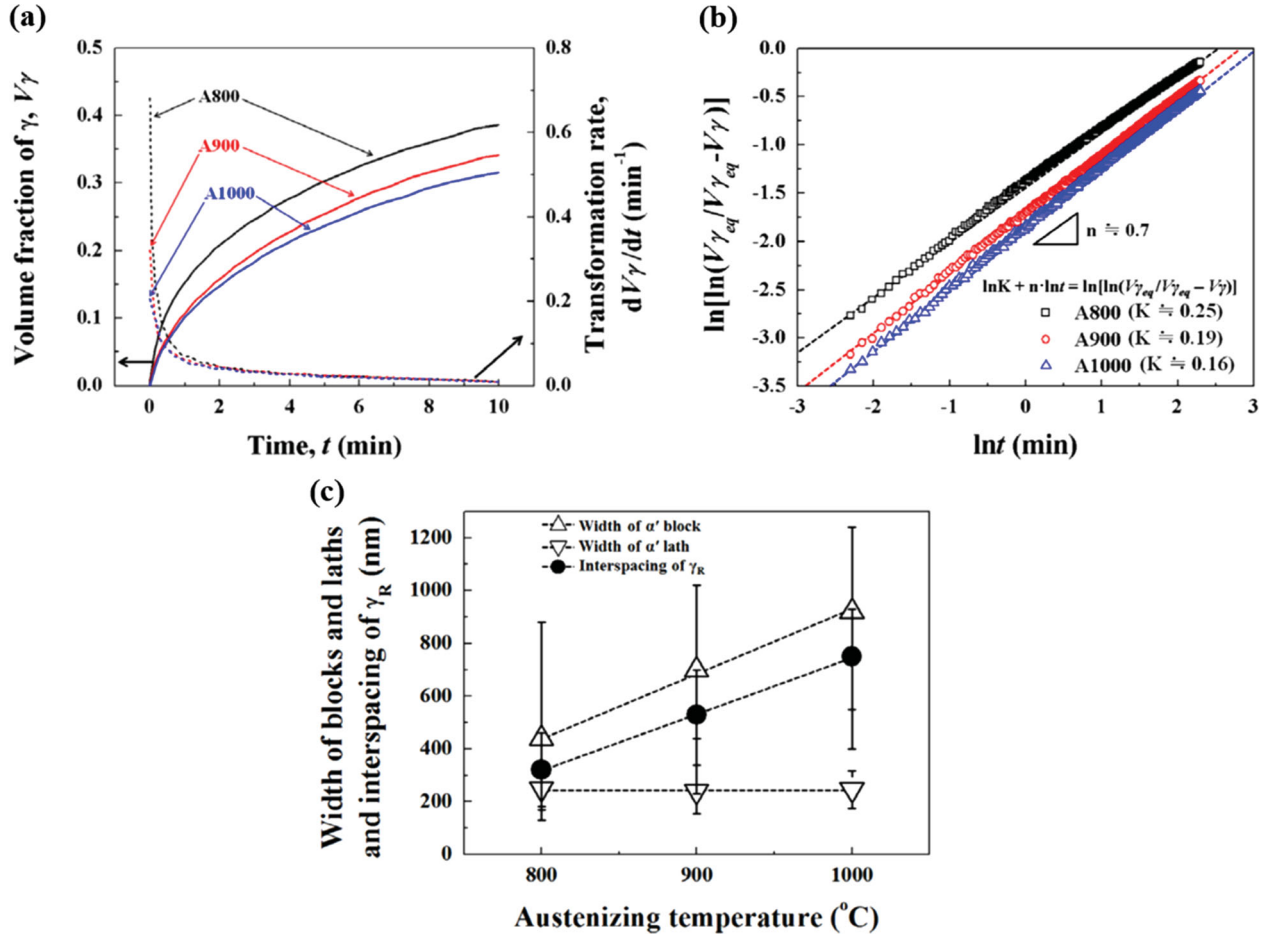

Figure 11. (a) Volume fraction and transformation rate of reverted austenite as a function of annealing time and austenitisation temperature; (b) $\ln[\ln(V_{\gamma\,eq}/V_{\gamma\,eq} - V_{\gamma})]$ — lnt plots of specimen austenitised at various temperatures; (c) dependence of the widths of the martensite blocks and laths, and the interspacing of retained austenite on the austenitisation temperature in Fe–9Mn–0.05C (wt-%) steel [23]. (Reproduced with permission from Elsevier).

area of martensite block boundaries, which provide nucleation sites for reverted austenite. The transformation rate of reverted austenite decreases with the increase in austenitising temperature, because of the lower boundary density of the prior austenite grains and the martensite constituents. The interspacing of the retained austenite laths becomes wider with increasing austenitising temperature, and it is similar to the width of the blocks [23].

4.2. The influence of the ART-annealing temperature

The annealing temperature has significant effects on the austenite volume fraction, stability of retained austenite and further the mechanical properties of medium-Mn steels. The influence of annealing temperature on the microstructure of Fe–7.9Mn–0.14Si–0.05Al–0.07C (wt-%) medium-Mn steel has been investigated [16]. Zhao et al. [16] reported that retained austenite volume fraction decreased with increasing annealing temperature from 600 to 700°C. The authors stated that the high annealing temperature results in high austenite fraction with low thermal stability during annealing. The austenite could transform into martensite during the cooling process.

Suh et al. [18] also reported that the annealing temperature had a great impact on the volume fraction and stability of retained austenite. Three alloys with different compositions have been investigated at various annealing temperatures. The result indicates that the retained austenite content does not differ significantly between the different alloys and the volume fraction increases gradually up to 760°C annealing temperature, but it dramatically drops for samples annealing at 780°C [18], as it is illustrated in Figure 12.

The reduced amount of retained austenite at high annealing temperature might be due to the following reasons: (1) An increasing annealing temperature can promote the formation and growth of austenite, resulting in an increase in austenite volume fraction during intercritical annealing. However, the larger the volume fraction of retained austenite is, the lower the amount of carbon and manganese in retained austenite is, thus, the high volume fraction of austenite formed at the annealing stage should associate with a weak stability. Consequently, more austenite might transform into ferrite or martensite during the subsequently cooling

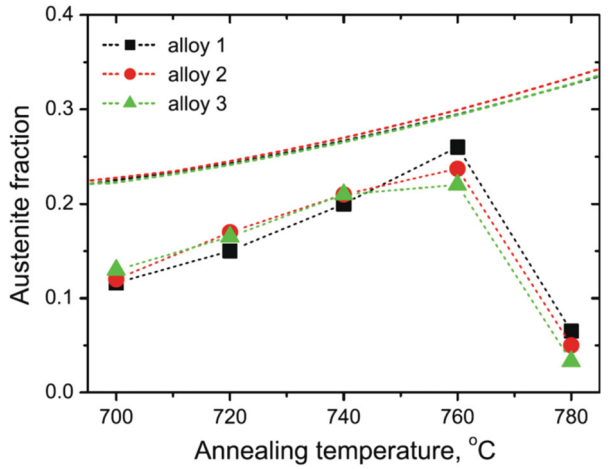

Figure 12. Dependence of austenite fraction in medium-Mn steels on the annealing temperature. The line without points represents the calculated equilibrium fractions [18]. Alloy 1: Fe–4.5Mn–2.2Al–0.45Si–0.11C (wt-%); Alloy 2: Fe–5.1Mn–2.1Al–0.49Si–0.075C (wt-%); Alloy 3: Fe–5.6Mn–2.2Al–0.49Si–0.055C (wt-%). (Reproduced with permission from Springer).

process [16, 18]. (2) High dislocation density created during rolling will remain in retained austenite at low temperature. The interstitial carbon atoms can easily segregate to dislocations in retained austenite, because they act as diffusion pipelines of carbon atoms. The carbon segregation results in the carbon content as high as 3––4 wt-% around the dislocations in retained austenite, thereby enhancing the retained austenite stability [16]. However, the dislocation density decreases at high annealing temperature, leading to the reduction in the diffusion channels.

Lee et al. [32] reported that the annealing temperature had a significant influence on the mechanical properties. With increasing of the annealing temperature in Fe-6wt-% Mn steel, the total elongation decreased, and the UTS increased. The highest strain hardening rate was obtained in the specimen annealed at 680°C. However, the Lüders deformation behaviour was found in the sample annealed at 640°C, indicating the absence of strain hardening. In order to understand the deformation behaviour, the austenite fractions before the tensile tests and after the tensile tests were measured. The results showed that no deformation-induced α'-martensite occurred during the deformation in the sample annealed at 640°C, however, austenite successively transformed into martensite during the tensile test in the sample annealed at 680°C.

The optimal intercritical annealing temperature for medium-Mn TRIP steel was suggested to be slightly lower than the TM temperature to avoid the presence of athermal martensite in the microstructure [21]. TM temperature is defined as the intercritical temperature for which the maximum volume fraction of austenite can be retained upon cooling to a room temperature [21].

The variation of yield strength, tensile strength and total elongation with different annealing temperatures are shown in Figure 13 [18]. The yield strength decreases with an increase in the annealing temperature, possibly because of the corresponding greater degree of softening (recovery and recrystallisation) of the initially cold-deformed ferrite at high temperature [18]. The tensile strength increases with the annealing temperature because the work hardening rates might be greatest for samples annealed at the highest of temperature (760°C) [18]. The largest volume fraction of retained austenite was obtained at 760°C in the studied medium-Mn steel [18]. However, the total elongation decreases with the increasing annealing temperature, which could be attributed to changes in the stability of the retained austenite [18]. Because the deformation-induced martensite plays a role in inducing more homogeneous deformation, there is an optimal austenite stability which is conducive to the late onset of necking during tensile tests.

4.3. The influence of the ART-annealing time

The influence of the annealing time on the duplex microstructure grain size has been studied for the cold-rolled Fe–5Mn–0.1C (wt-%) medium-Mn TRIP steel at an austenite-reverted-transformation temperature of 650°C [33]. It was mentioned that the austenite grain was about 0.4 μm after annealing for 1 min and coarsened slowly to approximately 1 μm after 6 h. The ferrite subgrain size was almost identical to the austenite grain size under the same annealing condition [33]. In the hot-rolled Fe–5Mn–0.2C (wt-%) steel annealed at 650°C [34], the thickness of austenite increased slightly from about 0.2 to 0.33 μm with the increase of annealing time from 1 to 48 h. The thickness of both austenite and ferrite laths remained smaller than 0.4 μm even after ART annealing at 650°C for 144 h, indicating the high thermal stability of the UFG duplex microstructure of medium-Mn TRIP steel. As shown in Figure 14 [35], it can be seen that there are two types of austenite grains after 1 min ART annealing at 650°C; one is the austenite lath that nucleated between the martensite laths, and the other one is the globular austenite, which probably formed at the prior austenite grain boundaries or the martensite packet boundaries [35]. The thickness of austenite lath increases slowly from about 0.1 μm to around 0.3 μm with increasing annealing time up to 12 h [35]. The authors concluded this might be attributed to the slow diffusion rate of Mn in austenite [35].

The experimental and modelling studies have indicated a logarithm dependence of austenite fraction on the intercritical annealing time up to 12 h in the Fe–5Mn–0.2C (wt-%) steel [35]. Then, the saturation of austenite fraction was reported for a longer annealing period [35]. However, too long annealing duration

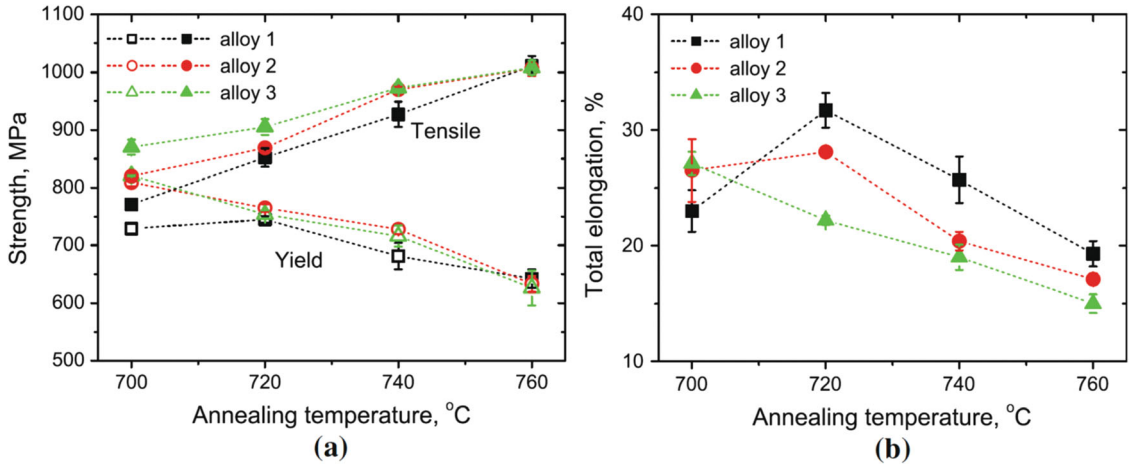

Figure 13. (a) Tensile and yield strength and (b) total elongation of annealed medium-Mn steels as a function of annealing temperature [18]. Alloy 1: Fe–4.5Mn–2.2Al–0.45Si–0.11C (wt-%); alloy 2: Fe–5.1Mn–2.1Al–0.49Si–0.075C (wt-%); alloy 3: Fe–5.6Mn–2.2Al–0.49Si–0.055C (wt-%). (Reproduced with permission from Springer).

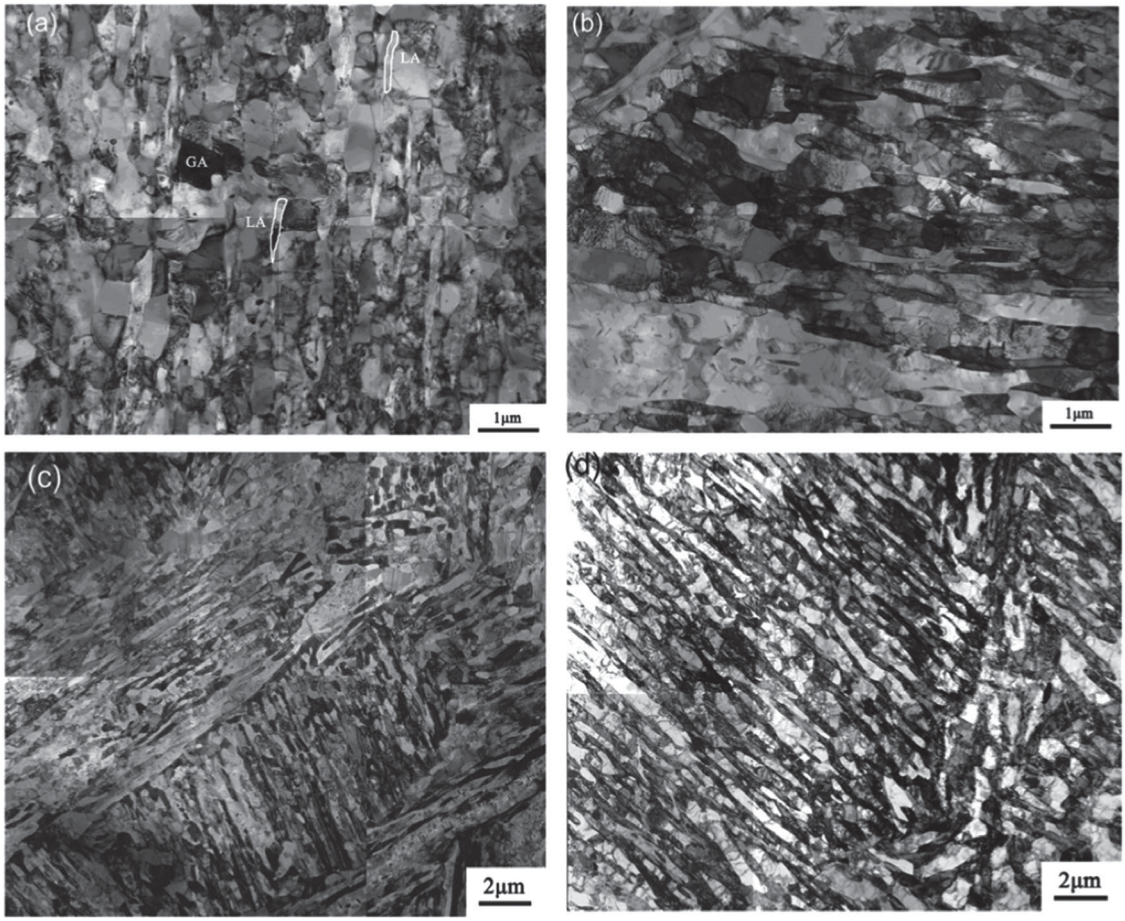

Figure 14. Microstructure of Fe–5Mn–0.2C (wt-%) steel after ART annealing at 650°C for different durations: (a) 1 min, (b) 5 min, (c) 1 h and (d) 12 h [35]. LA, lath austenite, GA, globular austenite. (Reproduced with permission from Springer).

should be avoided, because the austenite mechanical stability could be deteriorated and the total elongation and strength of the material could decrease [23].

4.4. The influence of the heating rate during ART annealing

The austenite reverted transformation was studied under the rapid heating rate (200°C s^{-1}) and short annealing time (2 s) condition [32]. It was found that a considerable amount of austenite was retained, regardless of the rapid heating rate and very short annealing time. It indicated that the austenite reverted transformation mode might be diffusionless in nature.

The recent study shows that the heating rate has an important effect on the austenite-reverted-transformation mechanism in Fe–9Mn–0.05C (wt-%) steel [36]. It is either diffusive or diffusionless

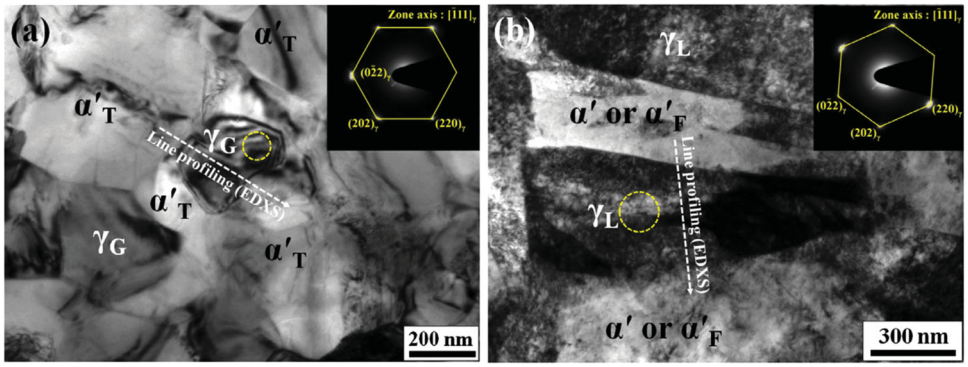

Figure 15. TEM bright field images of the Fe–9Mn–0.05C (wt-%) steel specimens annealed at (a) 645°C with a heating rate of 3°C s^{-1} and (b) 677°C with a heating rate of 50°C s^{-1}; both specimens were held for 10 s followed by quenching. γ_G is globular austenite, γ_L is lath-shape austenite, α'_T is tempered martensite, α'_F is fresh martensite, which is from the reverted austenite during quenching, and α' is untempered martensite [36]. (Reproduced with permission from Springer).

austenite-reverted-transformation mechanism due to the different heating rates during ART annealing. The morphologies of microstructures annealed at the low heating rate (3°C s^{-1}) and high heating rate (50°C s^{-1}) are shown in Figure 15(a) and (b), respectively [36].

According to the research by Han and Lee [36], when the specimens were slowly heated at rates below 15°C s^{-1}, cementite formed along various boundaries and then the reverted transformation from martensite to austenite occurred near the cementite particles. The critical temperatures for both cementite precipitation and the reverted transformation increased, as the heating rate increased up to 15°C s^{-1} [36]. They stated that slow heating rates resulted in a diffusive reversing transformation from quenched martensite to austenite [36]. During this low heating rate annealing process, the cementite precipitated at first and then dissolved in the matrix. A globular austenite with a low density of dislocations was formed during ART annealing. The diffusive reverted transformation might lead to pronounced manganese partitioning, which resulted in more stable retained austenite [36].

On the contrary, when the heating rate was greater than 15°C s^{-1}, rapid reverted transformation from martensite to austenite occurred without precipitation of the coarse and Mn-rich cementite [36]. This was due to the short time at high temperatures during the heating process, and the critical temperatures for the austenite reverted transformation were not significantly changed [36]. These results indicated that rapid heating rates caused the reverted transformation occur without diffusion. Diffusionless reverted specimens exhibited lath-shaped austenite grains with a high density of dislocations (shear-transformed phases) [36]. There was no pronounced manganese partitioning phenomenon at the early stage of the reverted transformation. It was presumed that further intercritical annealing could enhance the partition of both Mn and C atoms from α' (martensite) to γ_L (austenite lath), such that the thermal stability of γ_L gradually increased [36].

5. Conclusions

Medium-Mn steels exhibit an excellent balance of a cost-efficient alloy composition and mechanical properties, driving the innovation and development of the new grade of AHSS for automotive applications. ART annealing facilitates the enhanced austenite stability and the UFG austenite grain size in medium-Mn steels, leading to a considerable amount of retained austenite in the UFG microstructure down to room temperature. Medium-Mn steels processed by ART annealing manifest a good combination of high strength (UTS) from 800 to 1600 MPa and superior ductility from 20% to 65%.

Discontinuous yielding phenomenon characterises the UFG medium-Mn steels due to the absence of strain hardening. This localised deformation behaviour due to Lüders band propagation should be eliminated, particularly in the cold-rolled grade medium-Mn steels. The appearance of Lüders strains is accompanied by a poor surface quality. A precise control of the austenite stability and volume fraction of austenite enables the TRIP effect and TWIP effect during deformation, resulting in an improved strain hardening rate and enhanced mechanical properties.

It is essential to consider both extrinsic parameters, particularly the ART-annealing temperature, and intrinsic parameters, such as austenite fraction, austenite stability, grain size and SFE of UFG austenite at room temperature to obtain the desirable properties in medium-Mn steels. The increase of ART-annealing temperature in a suitable range results in the increased austenite fraction without much deterioration of austenite stability; meanwhile, the room temperature SFE of austenite is increased.

However, the previous studies have mainly focused on the improvement of tensile properties of this steel grade by adjustment of chemical composition and heat treatment parameters. For the industrialisation and application of medium-Mn steels, there are still lots of

properties needed to be further evaluated, like weldability, hole expansion ratio, sheet formability (forming limit diagram), dynamic tensile properties, delayed fracture properties, impact toughness, etc.

The two-step heat treatment process for cold-rolled medium-Mn steels (austenitisation and ART annealing) might not be compatible for the present steel manufactures. On the one hand, there exists only single-furnace continuous annealing line in most of the steel plants, which is not designed to perform the two-step annealing. On the other hand, hot-rolled strips with martensitic microstructure are unfavourable in the cold rolling process, which requests high load and power supply on the cold mill. Therefore, an additional annealing might be requested to soften the material before cold rolling, which is undesirable for industrial process. The hot rolling followed by the warm rolling might be an alternative manufacture process for the manufacture of medium-Mn steels.

Acknowledgements

The author gratefully acknowledges Professor Wolfgang Bleck, Dr Wenwen Song and Dr Xiaofei Guo for fruitful discussion. Some figures are reproduced with kind permission from Wiley-VCH Verlag GmbH & Co. KGaA (Figure 1), Elsevier (Figures 3, 8, 10, 11) and Springer (Figure 4, 6, 7, 9, 13, 14, 15).

Disclosure statement

No potential conflict of interest was reported by the author.

Funding

This work was supported by Deutsche Forschungsgemeinschaft (DFG) within the Collaborative Research Centre (SFB) 761 'Steel – *ab initio*'.

References

[1] Keeler S, Kimchi M. Advanced high-strength steels application guidelines V5. WorldAutoSteel; 2014.
[2] Matlock DK, Speer JG, De Moor E, et al. Recent development advanced high strength sheet steels for automotive applications: an overview. JESTECH. 2012;15:1–12.
[3] De Cooman BC, Kwon O, Chin KG. State-of-the-knowledge on TWIP steel. Mater Sci Technol. 2012;28:513–527.
[4] Billur E, Altan T. Three generations of advanced high-strength steels for automotive applications, Part I. Stamp J. 2013;Nov/Dec: 16–17.
[5] Song W, Prahl U, Bleck W. Steel—ab initio: quantum mechanics guided design of new Fe-based materials. Proceedings of the 3rd World Congress on Integrated Computational Materials Engineering (ICME2015), Colorado, USA; 2015 May–June; p. 47–54.
[6] Song W, Ingendahl T, Bleck W. Control of strain hardening behavior in high-Mn austenitic steels. Acta Metall Sin Engl Lett. 2014;27:546–556.
[7] Lan P, Zhang J. Thermophysical properties and solidification defects of Fe–22Mn–0.7C TWIP steel. Steel Res Int. 2016;87:250–261.
[8] Miller RL. Ultrafine-grained microstructures and mechanical properties of alloy steels. Metall Trans. 1972;3:905–912.
[9] Bleck W. Materials science of steel. Textbook. Aachen: IEHK; 2013.
[10] Arlazarov A, Gouné M, Bouaziz O, et al. Evolution of microstructure and mechanical properties of medium Mn steels during double annealing. Mater Sci Eng A. 2012;542:31–39.
[11] Wang C, Cao W, Shi J, et al. Deformation microstructures and strengthening mechanisms of an ultrafine grained duplex medium-Mn steel. Mater Sci Eng A. 2013;562:89–95.
[12] Zhang R, Cao WQ, Peng ZJ, et al. Intercritical rolling induced ultrafine microstructure and excellent mechanical properties of the medium-Mn steel. Mater Sci Eng A. 2013;583:84–88.
[13] Shi J, Sun X, Wang M, et al. Enhanced work-hardening behavior and mechanical properties in ultrafine-grained steels with large-fractioned metastable austenite. Scr Mater. 2010;63:815–818.
[14] Kim SJ. Effects of manganese content and heat treatment condition on mechanical properties and microstructures of fine-grained low carbon TRIP-aided steels. Mater Sci Forum. 2010;638–642:3313–3318.
[15] Han J, Lee SJ, Jung JG, et al. The effects of the initial martensite microstructure on the microstructure and tensile properties of intercritically annealed Fe–9Mn–0.05C steel. Acta Mater. 2014;78:369–377.
[16] Zhao X, Shen Y, Qiu L, et al. Effects of intercritical annealing temperature on mechanical properties of Fe–7.9Mn–0.14Si–0.05Al–0.07C steel. Materials. 2014;7:7891–7906.
[17] Lee S, De Cooman BC. Effect of the intercritical annealing temperature on the mechanical properties of 10 pct Mn multi-phase steel. Metall Mater Trans A. 2014;45:5009–5016.
[18] Suh DW, Ryu JH, Joo MS, et al. Medium-alloy manganese-rich transformation-induced plasticity steels. Metall Mater Trans A. 2013;44:286–293.
[19] Furukawa T, Huang H, Matsumura O. Effects of carbon content on mechanical properties of 5% Mn steels exhibiting transformation induced plasticity. Mater Sci Technol. 1994;10:964–970.
[20] De Moor E, Matlock DK, Speer JG, et al. Austenite stabilization through manganese enrichment. Scr Mater. 2011;64:185–188.
[21] Lee S, De Cooman BC. On the selection of the optimal intercritical annealing temperature for medium Mn TRIP steel. Metall Mater Trans A. 2014;44:5018–5024.
[22] Lee S, De Cooman BC. Tensile behavior of intercritically annealed ultra-fine grained 8% Mn multi-phase steel. Steel Res Int. 2015;86:1170–1178.
[23] Han J, Lee SJ, Lee CY, et al. The size effect of initial martensite constituents on the microstructure and tensile properties of intercritically annealed Fe–9Mn–0.05C steel. Mater Sci Eng A. 2015;633:9–16.
[24] Lee S, De Cooman BC. Tensile behavior of intercritically 10 pct Mn multi-phase steel. Metall Mater Trans A. 2014;45:709–716.
[25] Lee S, Woo W, De Cooman BC. Analysis of the tensile behavior of 12 pct Mn multi-phase ($\alpha+\gamma$) TWIP-TRIP steel by neutron diffraction. Metall Mater Trans A. 2016;47:2125–2140.

[26] Latypov MI, Shin S, De Cooman BC, et al. Micromechanical finite element analysis of strain partitioning in multiphase medium manganese TWIP+TRIP steel. Acta Mater. 2016;108:219–228.
[27] He BB, Luo HW, Huang MX. Experimental investigation on a novel medium Mn steel combining transformation- induced plasticity and twinning-induced plasticity effects. Int J Plast. 2016;78:173–186.
[28] Furukawa T. Dependence of strength-ductility characteristics on thermal history in low carbon, 5 wt.% Mn steels. Mater Sci Technol. 1989;5(5):465–470.
[29] Lee S, Estrin Y, De Cooman BC. Constitutive modeling of the mechanical properties of V-added medium manganese TRIP steel. Metall Mater Trans A. 2013;44:3136–3146.
[30] Lee S, Lee K, De Cooman BC. Observation of the TWIP+ TRIP plasticity-enhancement mechanism in Al-added 6 wt pct medium Mn steel. Metall Mater Trans A. 2015;46:2356–2363.
[31] Lee S, De Cooman BC. Annealing temperature dependence of the tensile behavior of 10 pct multi-phase TWIP-TRIP steel. Metall Mater Trans A. 2014;45:6039–6052.
[32] Lee S, Lee SJ, Kumar SS, et al. Localized deformation in multiphase, ultra-fine-grained 6 pct Mn transformation-induced plasticity steel. Metall Mater Trans A. 2011;42:3638–3651.
[33] Dong H, Cao W, Shi J. Formation of an ultrafine-grained austenite-containing microstructure from a cold-rolled medium-manganese steel processed using intercritical annealing. Mater Sci Forum. 2013;762:31–37.
[34] Wang C, Shi J, Wang CY, et al. Development of ultrafine lamellar ferrite and austenite duplex structure in 0.2C5Mn steel during ART-annealing. ISIJ Int. 2011;51:651–656.
[35] Luo H, Shi J, Wang C, et al. Experimental and numerical analysis on formation of stable austenite during the intercritical annealing of 5Mn steel. Acta Mater. 2011;59:4002–4014.
[36] Han J, Lee YK. The effects of the heating rate on the reverse transformation mechanism and phase stability of reverted austenite in medium Mn steels. Acta Mater. 2014;67:354–361.
[37] Sun R, Xu W, Wang C, et al. Work hardening behavior of ultrafine grained duplex medium-Mn steels processed by ART-annealing. Steel Res Int. 2012;83(4):316–321.
[38] Cao WQ, Wang C, Shi J, et al. Microstructure and mechanical properties of Fe–0.2C–5Mn steel processed by ART-annealing. Mater Sci Eng A. 2011;528:6661–6666.
[39] Xu HF, Zhao J, Cao WQ, et al. Heat treatment effects on the microstructure and mechanical properties of a medium manganese steel (0.2C–5Mn). Mater Sci Eng A. 2012;532:435–442.
[40] Xu HF, Zhao J, Cao WQ, et al. Tempering effects on the stability of retained austenite and mechanical properties in a medium manganese steel. ISIJ Int. 2012;52:868–873.
[41] Gibbs PJ, De Moor E, Merwin MJ, et al. Austenite stability effects on tensile behavior of manganese-enriched-austenite transformation-induced plasticity steel. Metall Mater Trans A. 2011;42(12):3691–3702.
[42] Zhao C, Zhang C, Cao WQ, et al. Variation of microstructure and mechanical properties of medium Mn steels with multiphase microstructure. Mater Sci Technol. 2016;32:63–70.
[43] Lee S, Lee K, De Cooman BC. Ultra fine-grained 6wt% manganese TRIP steel. Mater Sci Forum. 2010;654–656:286–289.
[44] Lee S-J, Lee S, De Cooman BC. Mn partitioning during the intercritical annealing of ultrafine-grained 6% Mn transformation-induced plasticity steel. Scr Mater. 2011;64:649–652.
[45] Lee S, Lee S-J, De Cooman BC. Austenite stability of ultrafine-grained transformation-induced plasticity steel with Mn partitioning. Scr Mater. 2011;65:225–228.
[46] Lee SJ, Lee S, De Cooman BC. Martensite transformation of sub-micron retained austenite in ultra-fine grained manganese transformation-induced plasticity steel. Int J Mater Res. 2013;104:423–429.
[47] Han J, Nam J-H, Lee Y-K. The mechanism of hydrogen embrittlement in intercritically annealed medium Mn TRIP steel. Acta Mater. 2016;113:1–10.
[48] Aydin H, Jung IH, Essadiqi E, et al. Twinning and Tripping in 10% Mn steels. Mater Sci Eng A. 2014;591:90–96.
[49] Su G, Gao X, Du L, et al. Influence of Mn on the corrosion behaviour of medium manganese steels in a simulated seawater environment. Int J Electrochem Sci. 2016;11:9447–9461.
[50] Tsuchiyama T, Inoue T, Tobata J, et al. Microstructure and mechanical properties of a medium manganese steel treated with interrupted quenching and intercritical annealing. Scr Mater. 2016;122:36–39.
[51] Lee S, Lee SJ, De Cooman BC. Work hardening behavior of ultrafine-grained Mn transformation-induced plasticity steel. Acta Mater. 2011;59:7546–7553.
[52] Luo H, Dong H, Huang M. Effect of intercritical annealing on the Lüders strain of medium Mn transformation-induced plasticity stees. Mater Des. 2015;83:42–48.
[53] Watté P, van Humbeeck J, Aernoudt E, et al. Strain ageing in heavily drawn eutectoid steel wires. Scr Mater. 1996;34:89–95.
[54] Leslie WC, Keh AS. Aging of flat-rolled steel products as investigated by electron microscopy. Mechanical working of steel II. New York(NY): Gorden and Breach; 1965. p. 337–377.
[55] Tsuchida N, Masuda H, Harada Y, et al. Effect of ferrite grain size on tensile deformation behavior of a ferrite-cementite low carbon steel. Mater Sci Eng A. 2008;488:446–452.
[56] Kusakin P, Belyakov A, Haase C, et al. Microstructure evolution and strengthening mechanisms of Fe–23Mn–0.3C–1.5Al TWIP steel during cold rolling. Mater Sci Eng A. 2014;617:52–60.
[57] Song W, Zhang W, von Appen J, et al. κ-phase formation in Fe–Mn–Al–C austenitic steels. Steel Res Int. 2015;86:1161–1169.